Electrochimica Acta 55 (2010) 7945–7950

Contents lists available at ScienceDirect

Electrochimica Acta

journal homepage: www.elsevier.com/locate/electacta

Cobalt based non-precious electrocatalysts for oxygen reduction reaction in proton exchange membrane fuel cells

Yuanwei Ma[a,b], Huamin Zhang[a,*], Hexiang Zhong[a], Ting Xu[a,b], Hong Jin[a,b], Yongfu Tang[a,b], Zhuang Xu[a,b]

[a] PEMFC Key Materials and Technology Laboratory, Dalian Institute of Chemical Physics, Chinese Academy of Sciences, No. 457 Zhongshan Road, Dalian 116023, China
[b] Graduate School of the Chinese Academy of Sciences, Beijing 100039, China

ARTICLE INFO

Article history:
Received 31 October 2009
Received in revised form 25 March 2010
Accepted 26 March 2010
Available online 2 April 2010

Keywords:
Proton exchange membrane fuel cells
Non-precious metal catalyst
Electrocatalyst
Oxygen reduction reaction
Nanocomposite

ABSTRACT

Cobalt based non-precious metal catalysts were synthesized using chelation of cobalt (II) by imidazole followed by heat-treatment process and investigated as a promising alternative of platinum (Pt)-based electrocatalysts in proton exchange membrane fuel cells (PEMFCs). Transmission electron microscopy (TEM), X-ray diffraction (XRD) and X-ray photoelectron spectroscopy (XPS) measurements were used to characterize the synthesized CoN_x/C catalysts. The activities of the catalysts towards oxygen reduction reaction (ORR) were investigated by electrochemical measurements and single cell tests, respectively. Optimization of the heat-treatment temperature was also explored. The results indicate that the as-prepared catalyst presents a promising electrochemical activity for the ORR with an approximate four-electron process. The maximum power density obtained in a H_2/O_2 PEMFC is as high as 200 mW cm^{-2} with CoN_x/C loading of 2.0 mg cm^{-2}.

1. Introduction

Proton exchange membrane fuel cells (PEMFCs) have received wide attention over the recent few decades as an environmental benign technology, because of low emissions and high conversion efficiency for vehicle and portable devices. As one of the key materials in PEMFCs, electrocatalysts is crucially important to the development of PEMFCs. Up to now, Pt/C is regarded as the most active catalyst for the oxygen reduction reaction (ORR), but its limited availability and high cost hinder the further commercialization of the PEMFCs.

Many efforts have been made to lower the cost of electrocatalysts. Among those, alloys of Pt and transition metals such as Fe [1], Co [2,3], Ni [4], Cr [5], etc. are the generally used way. The Pt-based alloys demonstrate higher catalytic activity compared with pure Pt metal [1–5]. Another method is to develop core–shell catalyst [6–8] by arranging Pt as the thin shells, which reduces the amount of Pt. Although these two major methods have decreased the Pt loading, the overall cost is expensive. Furthermore, the limited resource of Pt, which cannot be resolved, is the key issue hampers the final application of the fuel cells. Thus, to scale-up this technology, developing non-precious metal catalysts would be a final solution [9]. Hence alternative materials to Pt electrocatalysts need to be explored.

Since Jasinski found that Co-phthalocyanine exhibited catalytic activity towards the ORR [10], a number of transition metal macrocycles have been developed as cathode catalysts for the ORR. However, poor stability in acidic media is the major disadvantage of this kind of catalyst [11,12]. It was reported that the stability can be greatly improved by using heat-treatment. This can be attributed to less production of hydrogen peroxide during the ORR process, which attacks the active site [13,14].

Generally, transition metal macrocycles catalysts were prepared by impregnation of a transition metal N_4-chelate precursor onto carbon black, followed by heat-treatment under inert atmosphere [15–17]. However, the transition metal macrocycles were still somewhat expensive. Alternative synthesis routes that aimed to prepare catalysts with similar active surface species which were formed during the heat-treatment of transition metal chelates that utilized cheap nitrogen-containing precursors and transition metal containing precursors had been explored [18]. Up to now, many nitrogen-containing precursors have been used to prepare transition metal macrocycles, such as phthalocyanine [19], perylene tetracarboxylic dianhydride [20], ammonia [21], polypyrrole [22], and ethylene diamine [23].

In this work, a new non-precious metal was studied to address the activity and cost issues. The catalysts were prepared by using a chelation process with cobaltous nitrate and imidazole as simple

* Corresponding author. Tel.: +86 411 84379072; fax: +86 411 84665057.
E-mail address: zhanghm@dicp.ac.cn (H. Zhang).

0013-4686/$ – see front matter © 2010 Elsevier Ltd. All rights reserved.
doi:10.1016/j.electacta.2010.03.087

Co and N precursors. The main reason for using imidazole is to imitate the atomic configuration of Co-porphyrins [22,24]. Here, imidazole is introduced for entrapping cobalt due to its high N atom content. With simple structure without any side-chains, there may be lesser steric hindrance for imidazole to form Co–N sites, thus forming active ORR sites. The as-prepared catalysts were characterized by transmission electron microscopy (TEM), X-ray diffraction (XRD) and X-ray photoelectron spectroscopy (XPS) measurements. The ORR activities of the catalysts were studied in detail by electrochemical measurement and single cell test.

2. Experimental

2.1. Electrocatalysts preparation

CoN_x/C catalyst was prepared as follows: 197.3 mg $Co(NO_3)_2{\cdot}6H_2O$ and 160 mg imidazole were dissolved in 50 mL ethanol followed by stirring at 60 °C to form a Co–N complex. Then, 200 mg Black Pearls 2000 carbon black powders (Carbot Corp., $S_{BET} = 1500\ m^2\ g^{-1}$) were added into the solution. The mixture was stirred vigorously for 5 h and dried under vacuum at 60 °C for 8 h. The resulting powder samples were heat-treated in N_2 atmosphere at different temperatures ranging from 600 to 900 °C. The as-prepared catalysts were denoted as CoN_x/C.

2.2. Physicochemical characterizations

TEM images were recorded on JEOL JEM-2000EX microscope operated at 120 kV. The catalyst was placed in a vial containing ethanol. The sample was agitated in ultrasonic bath to form homogeneous slurry. A drop of the slurry was dispersed on a holey, amorphous carbon film on a Cu grid for analysis.

XRD analysis of the samples was performed on a Rigaku Rotalflex (RU-200B) using Cu Kα radiation (λ = 1.54056 Å) with a Ni-filter to characterize the CoN_x/C crystalline structures. The 2θ angular region extended from 20° to 80°, and the scan rate was 5° min^{-1} with a step size of 0.02°.

XPS data were acquired using Mg Kα radiation (1253.6 eV) with a power of 200 W and pass energy of 50 eV. The deconvolution of XPS peak was conducted by a Lorentzian–Gaussian function.

2.3. Electrochemical measurements

Eletrochemical measurements were performed on CHI 600 electrochemical station with a rotating disk electrode (RDE) system (EG&G model 636). A standard three-electrode electrochemical cell was used. All the electrochemical measurements were carried out in 0.5 M H_2SO_4 solution at room temperature with a saturated calomel electrode (SCE) and a large-area Pt foil (3 cm^2) as the reference electrode and the counter electrode, respectively. The catalyst layer on the glassy carbon electrode (GCE) (0.1256 cm^2) was prepared as follows. A mixture containing 5.0 mg CoN_x/C or Pt/C (20 wt.%, Johnson Matthey) catalysts, 50 μL Nafion solution (5 wt.%, Du Pont Corp.) and 1.0 mL ethanol was blended in ultrasonic bath in a weighing bottle for 30 min to obtain a homogeneous ink. A 12.5 μL paint ink was spread onto the surface of a GCE and the electrode was dried in the air to obtain a thin catalyst layer. The loading of catalysts were 0.47 mg cm^{-2}. The CV curves were obtained in the potential range from −0.24 to 0.96 V versus SCE with the scan rate of 50 mV s^{-1} under N_2 atmosphere. The RDE curves were obtained in the potential range of −0.2 to 0.90 V versus SCE with the scan rate of 5 mV s^{-1} at room temperature. Before the RDE tests, the electrolyte was saturated with O_2 by bubbling O_2 for 30 min.

The rotating ring disk electrode (RRDE) measurements were performed in a three-electrode electrochemical cell using VMP3 electrochemical station (Princeton Applied Research) at room temperature. An RRDE with Pt ring (6.25 mm inner-diameter and 7.92 mm outer-diameter) and glassy carbon disk (5.61 mm diameter) was employed as the working electrode. The catalyst ink was prepared by the same way as mentioned above. A 25 μL CoN_x/C paint ink was spread on the surface of a glassy carbon disk to keep the same catalyst loading as RDE measurement. The electrolyte was 0.5 M H_2SO_4 solution. A platinum mesh and a SCE were used as the counter and reference electrodes, respectively. The disk potential was the same as RDE measurement. After the activation step, the ring potential was held at 0.9 V versus SCE. All electrode potentials in this paper were quoted to reversible hydrogen electrode (RHE).

2.4. Membrane electrode assembly (MEA) fabrication and single cell tests

The electrode was prepared as follows. A mixture containing CoN_x/C or Pt/C (20 wt.%, Johnson Matthey) catalysts, 5% Nafion (Du Pont Corp.) was blended in ultrasonic bath in a weighing bottle for 30 min to obtain a homogeneous ink. Then, the mixture was cast onto the prefabricated gas diffusion layer (Torry carbon paper as substrate, 7 wt.% PTFE). This as-fabricated electrode was used as the cathode. The anode adopted the commercial Pt/C catalyst (TKK Corp.) with Pt loading of 0.3 mg cm^{-2}. The dry Nafion loading in the anode was about 0.4 mg cm^{-2}. The MEA was fabricated by hot-pressing the anode and the cathode sandwiching the Nafion 212 membrane (50 μm, Du Pont Corp.) at 140 °C and 1 MPa for 1 min. The MEA active area was 5 cm^2. The single cell performances were tested at 80 °C with saturated humidification. The single cell was fed with pure hydrogen and oxygen and operated at 0.2 MPa.

3. Results and discussion

3.1. Electrochemical measurements

Fig. 1 displays the ORR polarization curves for CoN_x/C catalysts heat-treated at various temperatures from 600 to 900 °C in O_2-saturated 0.5 M H_2SO_4 solution at room temperature, with the CoN_x/C unheat-treatment (UT) and commercial Pt/C (20 wt.%, Johnson Matthey) catalysts as the comparison. The results demonstrate that the catalytic activity strongly depends on the condition of heat-treatment. As shown in Fig. 1, the CoN_x/C catalyst before heat-treatment presents lowest activity towards ORR. With the increase of heat-treatment temperature, the catalytic activity is enhanced at the beginning and slightly decreases with further increasing of

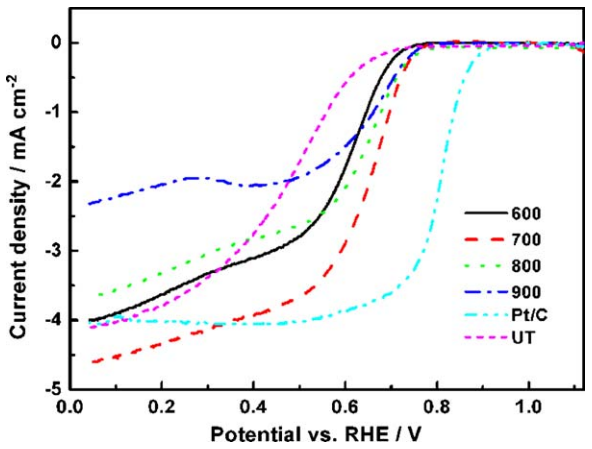

Fig. 1. Polarization curves on rotating disk electrode for CoN_x/C catalysts heat-treated at 600–900 °C in 0.5 M H_2SO_4 solution saturated with oxygen. Potential scan rate: 5 mV s^{-1}; rotation speed: 1600 rpm.

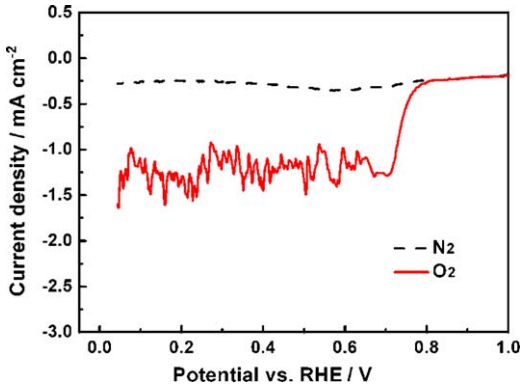

Fig. 2. Polarization curves on rotating disk electrode for CoN_x/C catalysts heat-treated at 700 °C in 0.5 M H_2SO_4 solution saturated with nitrogen or oxygen. Potential scan rate: 5 mV s^{-1}; rotation speed: 0 rpm.

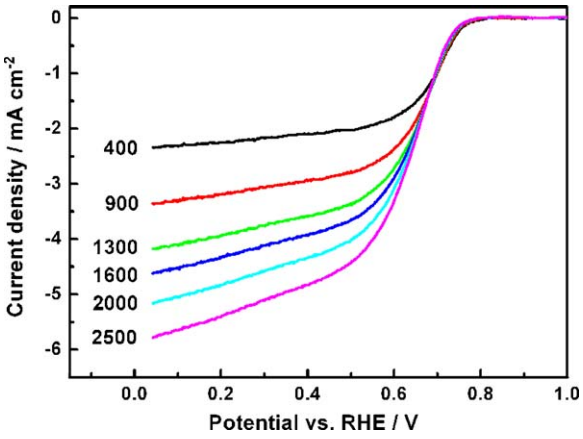

Fig. 3. Rotating disk electrode measurements for oxygen reduction on CoN_x/C catalyst heat-treated at 700 °C in 0.5 M H_2SO_4 solution saturated with oxygen. Potential scan rate: 5 mV s^{-1}; disk area: 0.1256 cm^2; rotating speeds are indicated in the figure.

temperature. The highest activity is obtained for the catalyst heat-treated at 700 °C. The reason for higher activity of the catalyst heat-treat at 700 °C may be the formation of the N-containing fragments [25,26], which is active towards ORR. Compared with Pt/C, the diffusion-limited plateau of the polarization curves for CoN_x/C catalysts is not very clear. It was reported [27] that the plateau is more inclined when the distribution of active site is less uniform and the reaction is slower. Although it shows about 150 mV higher overpotential for oxygen reduction in comparison with Pt/C catalyst, among various temperatures the CoN_x/C catalyst heat-treated at 700 °C shows the higher activity for both activation overpotential and the reaction kinetics towards ORR. Therefore, the catalyst heat-treated at 700 °C was selected to study in detail.

Fig. 2 illustrates the polarization curves for the CoN_x/C catalyst at N_2 and O_2 atmosphere, respectively. As shown in Fig. 2, the reduction current with CoN_x/C catalyst increases sharply at O_2 atmosphere, compared with that at N_2 atmosphere. This reduction current should be attributed to the oxygen reduction. The onset potential for the ORR on CoN_x/C catalyst prepared in this work is about 0.81 V versus RHE, which is comparable to CoTETA/C of 0.78 V versus RHE by Zhang et al. [28] and CoEDA/C of 0.82 V versus RHE by Subramanian et al. [29], respectively. As a non-precious metal catalyst, CoN_x/C prepared in this work, which shows about 100 mV lower onset potential in comparison with Pt/C catalyst, indicates high activity towards ORR.

It is known that the ORR can proceed by two main routes in an acidic solution [30]: the direct four-electron reduction to produce water through reaction (1); or the two-electron reduction to produce hydrogen peroxide through reaction (2), which can be further reduced to water through reaction (3). A desired catalyst for ORR would reduce oxygen molecules to water through the four-electron route. H_2O_2 produced in two-electron process is the primary cause of the degradation of the catalytic site, causing poor stability [13,14].

$$O_2 + 4H^+ + 4e^- \rightarrow 2H_2O; \quad E^0 = 1.229\,\text{V vs.NHE} \tag{1}$$

$$O_2 + 2H^+ + 2e^- \rightarrow H_2O_2; \quad E^0 = 0.67\,\text{V vs.NHE} \tag{2}$$

$$H_2O_2 + 2H^+ + 2e^- \rightarrow 2H_2O; \quad E^0 = 1.77\,\text{V vs.NHE} \tag{3}$$

To verify the oxygen reduction mechanism of CoN_x/C, the Koutecky–Levich equation [31] was used to determine the number of electrons transferred per O_2 molecule.

$$-\frac{1}{I} = -\frac{1}{I_k} + \frac{1}{0.62nFAD^{2/3}c\nu^{-1/6}\omega^{1/2}} \tag{4}$$

where I_k is the kinetic current; ω is the rotation rate; n is the number of electrons involved in the reaction; F is Faraday constant; A is the geometric area of the disk electrode; D and c are the diffusion coefficient of dissolved oxygen and the concentration of dissolved oxygen in 0.5 M H_2SO_4, respectively; ν is the kinematic viscosity of the electrolyte. Fig. 4 shows Koutecky–Levitch (I^{-1} versus $\omega^{-1/2}$) plots for the ORR on CoN_x/C electrodes at different electrode potentials in 0.5 M H_2SO_4. The number of electrons transferred per O_2 molecule was determined by Eq. (4) according to the data in Fig. 3. The linearity of the plots confirmed the applicability of Eq. (4) to analysis of the behavior at the electrocatalyst layer. The calculation of n was performed using the values: F, 96,485 C mol^{-1}; A, 0.1256 cm^2; D, 1.93×10^{-5} cm^2 s^{-1}; c, 1.13×10^{-6} mol cm^{-3}; ν, 9.5×10^{-3} cm^2 s^{-1} [32]. The number of electrons is 3.6, close to 4. This suggests that the molecular oxygen is reduced to water on the surface of CoN_x/C in an approximate four-electron process.

The RRDE technique was performed to determine the catalytic activity and selectivity to four-electron oxygen reduction as shown in Fig. 5. The equations used to calculate n (the apparent number of electrons transferred during ORR) and % H_2O_2 (the percentage of H_2O_2 released during ORR) are as follows [33–35]:

$$\%H_2O_2 = 100 \times \frac{2I_r}{NI_d + I_r} \tag{5}$$

$$n = \frac{4I_d}{I_d + (I_r/N)} \tag{6}$$

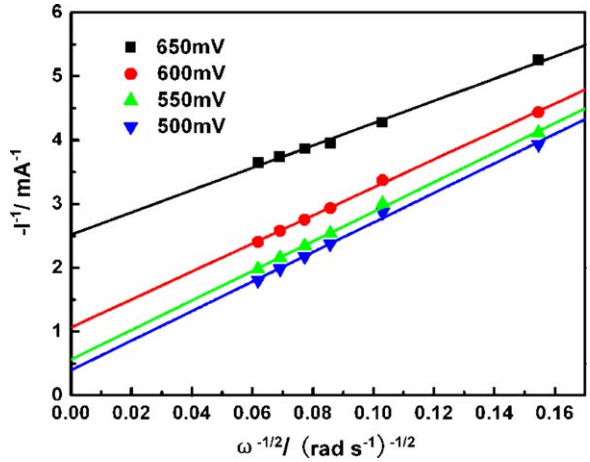

Fig. 4. Levich–Koutecky plots for oxygen reduction on CoN_x/C in 0.5 M H_2SO_4 solution saturated with oxygen obtained from the data in Fig. 3.

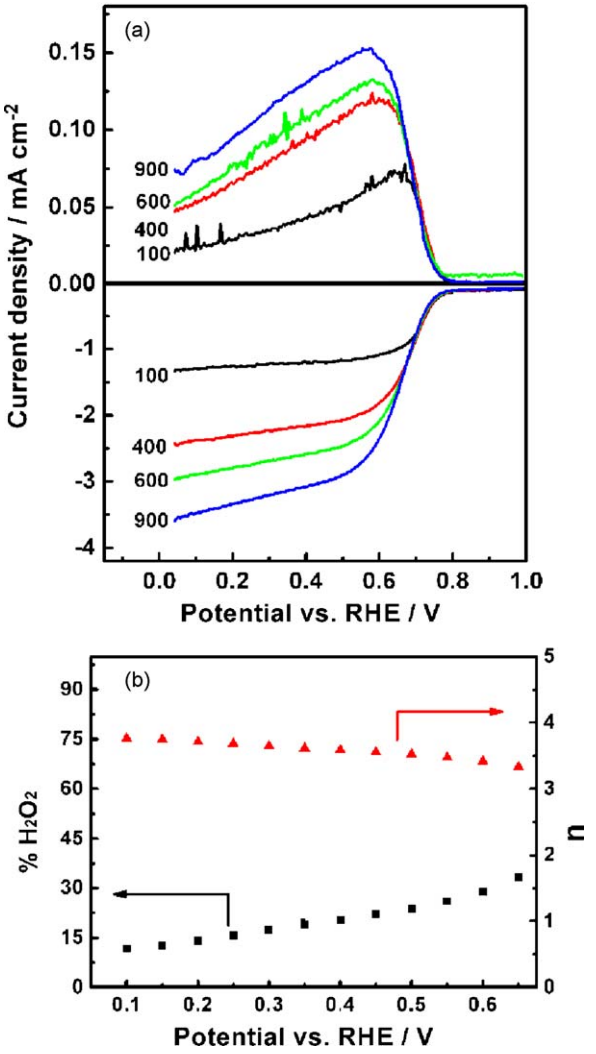

Fig. 5. (a) Rotating ring disk electrode measurements for oxygen reduction on CoN_x/C catalyst heat-treated at 700 °C in 0.5 M H_2SO_4. Potential scan rate: 5 mV s^{-1}; disk area: 0.2475 cm^2; rotating speed are indicated in the figure; (b) potential–% H_2O_2 curve and potential–*n* curve for CoN_x/C catalyst heat-treated at 700 °C with rotation speeds of 900 rpm.

where I_d is the Faradaic current at the disk, I_r is the Faradaic current at the ring and $N = 0.37$ is the RRDE collection efficiency. This method is convenient when observed disk currents do not level off, as it is often the case for non-noble metal based catalysts [36]. As shown in Fig. 5(b), % H_2O_2 was calculated to be 11.8–33.4 according to Eq. (5). And *n* (the number of electrons transferred) was calculated to be 3.3–3.8 according to Eq. (6). These suggest that the molecular oxygen is mostly reduced to water directly on the surface of CoN_x/C, which is in well agreement with the results of RDE measurements.

3.2. Characterizations of the electrocatalysts

Fig. 6 shows the XRD patterns of CoN_x/C catalysts before heat-treatment and heat-treated at 700 °C, respectively. Two 2θ crystalline peaks could be observed at 44.3° and 51.6°, respectively after heat-treatment, while there was no obvious peak for the sample before heat-treatment. The two peaks observed for the heat-treated CoN_x/C could be assigned as β-Co metal [17,25,37]. This indicates that during the heat-treatment process some ionic Co is reduced to form metallic Co on the carbon support.

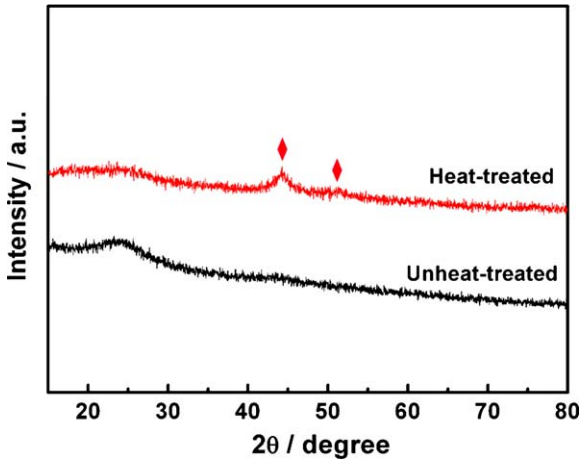

Fig. 6. XRD patterns of CoN_x/C catalysts.

In this work, the surface characterization of CoN_x/C catalysts before and after heat-treatment was characterized by XPS. Fig. 7 illustrates XPS peaks of N 1s for CoN_x/C catalysts.

As shown in Fig. 7(a), for the unheat-treated CoN_x/C catalyst, there are four peaks for N 1s at 397.5, 398.8, 400.0 and 404.9 eV, respectively. The main peak at 397.5 eV could be assigned to N in imidazole, nonbonding to H [38]. The N peak at 398.8 eV could be assigned to Co–N bond [38], which is the bonding between the imidazole nitrogens and the Co ion. The N peak at 400.0 eV could be

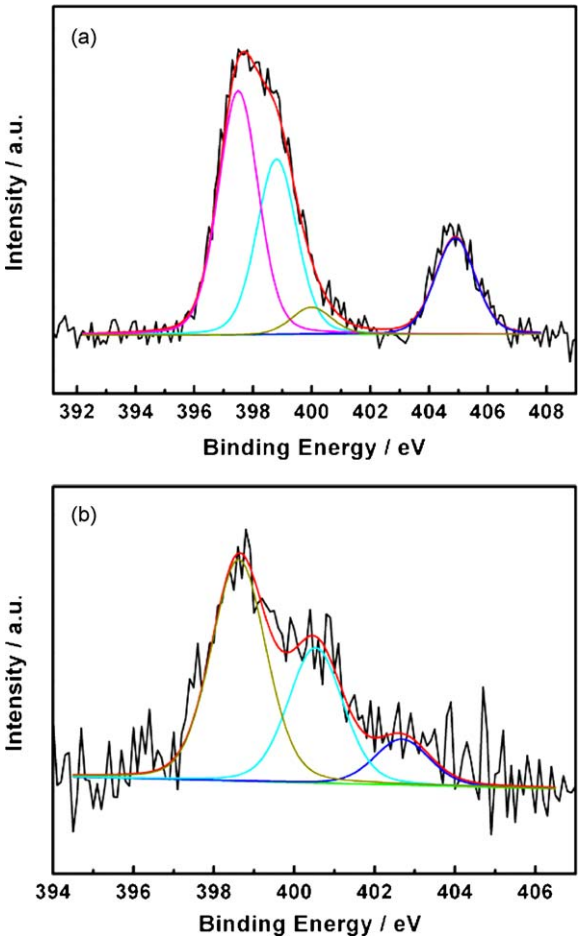

Fig. 7. XPS spectra of CoN_x/C for N 1s core-level peaks: (a) unheat-treated and (b) heat-treated at 700 °C.

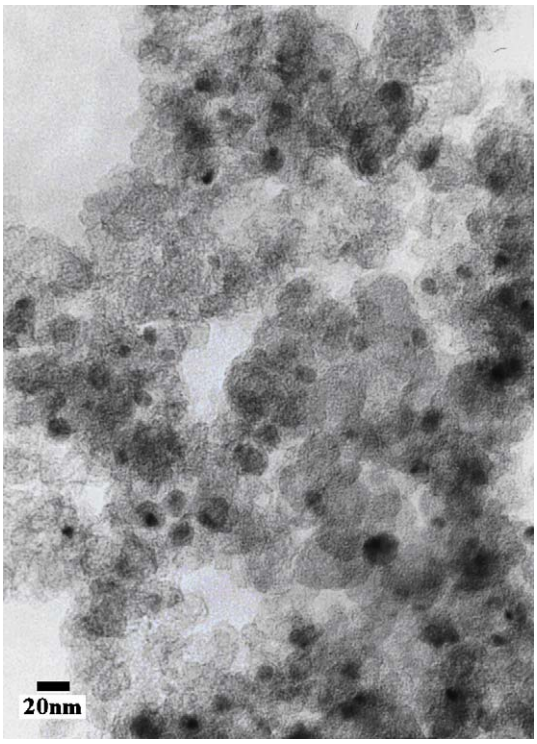

Fig. 8. TEM image of CoN_x/C catalyst.

assigned to N–H bond in imidazole [38,39]. The N peak at 404.9 eV could be assigned to N in $-NO_3$. As shown in Fig. 1, the CoN_x/C catalyst before heat-treatment indicates some activity towards ORR. The activity may be attributed to Co–N bond, because imidazole has no activity towards ORR.

As shown in Fig. 7(b), for the spectra of the catalyst heat-treated at 700 °C, three peaks for N 1s are observed at 398.6, 400.5 and 402.7 eV, respectively. The peak observed at 400.5 eV corresponds to pyrrolic N which is bonded to two carbon atoms at the edge of a graphene layer contributing to the π band with two electrons [40]. The peak appeared at 402.7 eV corresponds to graphitic N which is bounded to three carbon atoms in different locations in the center of the graphene layer [40]. The main peak appeared at 398.6 eV can be assigned to Co–N bond which has not decomposed after heat-treatment or pyridinic N which is bonded to two carbon atoms of the graphene layer donating one p electron to the aromatic π system [39]. Since these two different N have the same XPS peak position, it is very difficult to distinguish between them exactly [39]. The main peak at 398.6 eV occupies a majority of portion (~55 at.%) of the total surface nitrogen, which is probably contributed by both Co–N and pyridinic N, may act as catalytic sites, and contribute to the high activity of the catalyst and the approximate four-electron process.

Fig. 8 shows TEM image of CoN_x/C catalyst heat-treated at 700 °C. Some black particles were observed on the carbon support in the CoN_x/C sample. Most probably that these particles are attributed to the β-Co phase aggregated on the carbon support surface, which is consistent with the observation from the XRD analysis in Fig. 7.

3.3. Single cell tests

Fig. 9 shows performances of single cell using CoN_x/C catalyst heat-treated at 700 °C as cathode, with the commercial Pt/C (20 wt.%, Johnson Matthey) catalyst as the comparison. Polarization curves of CoN_x/C demonstrate open circuit voltage (OCV) at

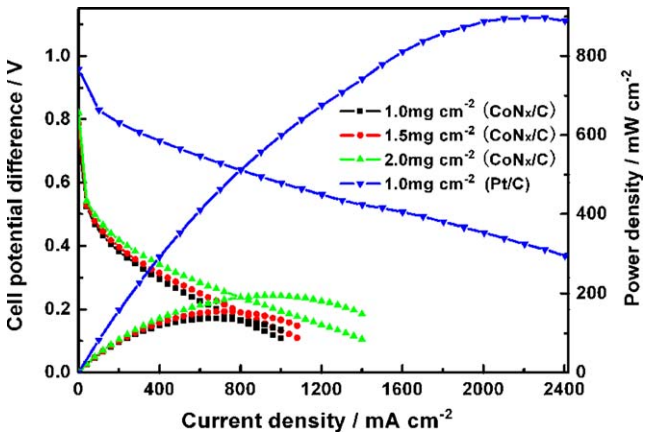

Fig. 9. Polarization curves of single cells with different loadings of cathode catalysts.

about 0.74–0.82 V, which is lower than that of Pt/C catalyst (0.96 V). The possible reason for comparatively low OCV is partly due to the extrapolarization caused by relatively lower ORR activity of CoN_x/C catalyst [41]. It also can be observed that the cell performance is enhanced with catalyst loading increased from 1.0 to 2.0 mg cm^{-2}. The improved cell performance could be due to an increase of active sites with high catalyst loading. The maximum power density of single cell with CoN_x/C loading of 2.0 mg cm^{-2} is approximate 200 mW cm^{-2}. Although the maximum power density of CoN_x/C catalyst is only one fourth of Pt/C, it still has significance to do further study due to its low price, abundant resources and scientific research reasons. And it is expected to be a promising non-Pt cathode electrocatalyst for PEMFCs.

4. Conclusions

Cobalt based non-precious metal catalysts were synthesized by using a chelation process and explored as a cathode catalyst for oxygen reduction reaction (ORR) in PEMFCs. The results indicate that the non-precious catalyst presents a promising electrocatalytic activity for the ORR with an approximate four-electron process. The catalytic activity strongly depends on the condition of heat-treatment. Among various heat-treatment temperatures, CoN_x/C catalyst heat-treated at 700 °C presents the highest activity towards the ORR. The optimized catalyst exhibits an onset potential for ORR as high as 0.81 V versus RHE. In single cell test, the maximum power density with the catalyst as cathode is about 200 mW cm^{-2} at 80 °C. The catalytic activities of CoN_x/C are believed to have broad development space with further optimizations in both the catalyst preparation process and MEA manufacture. This future work will focus on ways to reduce Co phase aggregated on the carbon support, thus making the distribution of active site more uniform and accelerating the reaction. It is expected to be a promising non-Pt cathode electrocatalyst for PEMFCs because of its low cost and desirable activity.

Acknowledgements

The authors gratefully acknowledge for financial support by the National High Technology Research and Development Program of China (863 Program), No. 2009AA05Z114.

References

[1] V. Baglio, A.S. Aricò, A. Stassi, C. D'Urso, A. Di Blasi, A.M. Castro Luna, V. Antonucci, J. Power Sources 159 (2006) 900.
[2] E.I. Santiago, L.C. Varanda, H.M. Villullas, J. Phys. Chem. C 111 (2007) 3146.
[3] J.R.C. Salgado, E. Antolini, E.R. Gonzalez, J. Phys. Chem. B 108 (2004) 17767.

[4] V. Stamenkovic, T.J. Schmidt, P.N. Ross, N.M. Markovic, J. Phys. Chem. B 106 (2002) 11970.
[5] H. Yang, N. Alonso-Vante, J.M. Léger, C. Lamy, J. Phys. Chem. B 108 (2004) 1938.
[6] S. Guo, Y. Fang, S. Dong, E. Wang, J. Phys. Chem. C 111 (2007) 17104.
[7] Y. Chen, F. Yang, Y. Dai, W. Wang, S. Chen, J. Phys. Chem. C 112 (2008) 1645.
[8] J. Zhang, F.H.B. Lima, M.H. Shao, K. Sasaki, J.X. Wang, J. Hanson, R.R. Adzic, J. Phys. Chem. B 109 (2005) 22701.
[9] C.W.B. Bezerra, L. Zhang, K. Lee, H. Liu, A.L.B. Marquesc, E.P. Marques, H. Wang, J. Zhang, Electrochim. Acta 53 (2008) 4937.
[10] R. Jasinski, Nature 201 (1964) 1212.
[11] L. Zhang, J. Zhang, D.P. Wilkinson, H. Wang, J. Power Sources 156 (2006) 171.
[12] C.W.B. Bezerra, L. Zhang, H. Liu, K. Lee, A.L.B. Marques, E.P. Marques, H. Wang, J. Zhang, J. Power Sources 173 (2007) 891.
[13] B. Wang, J. Power Sources 152 (2005) 1.
[14] H. Liu, C. Song, Y. Tang, J. Zhang, J. Zhang, Electrochim. Acta 52 (2007) 4532.
[15] H. Kalvelage, A. Mecklenburg, U. Kunz, U. Hoffmann, Chem. Eng. Technol. 23 (2000) 9.
[16] P. Gouérec, M. Savy, Electrochim. Acta 44 (1999) 2653.
[17] G. Lalande, R. Côté, G. Tamizhmani, D. Guay, J.P. Dodelet, L. Dignard-Bailey, L.T. Weng, P. Bertrand, Electrochim. Acta 40 (1995) 2635.
[18] S. Gupta, D. Tryk, I. Bae, W. Aldred, E. Yeager, J. Appl. Electrochem. 19 (1989) 19.
[19] R. Côté, G. Lalande, D. Guay, J.P. Dodelet, G. Dénès, J. Electrochem. Soc. 145 (1998) 2411.
[20] M. Lefèvre, J.P. Dodelet, J. Phys. Chem. B 106 (2002) 8705.
[21] M. Lefèvre, J.P. Dodelet, J. Phys. Chem. B 104 (2000) 11238.
[22] R. Bashyam, P. Zelenay, Nature 443 (2006) 63.
[23] V. Nallathambi, J.W. Lee, S.P. Kumaraguru, G. Wu, B.N. Popov, J. Power Sources 183 (2008) 34.
[24] C. Fierro, A.B. Anderson, D.A. Scherson, J. Phys. Chem. 92 (1988) 6902.
[25] G. Faubert, G. Lalande, R. Côté, D. Guay, J.P. Dodelet, L.T. Weng, P. Bertrand, G. Dénès, Electrochim. Acta 41 (1996) 1689.
[26] M. Lefèvre, J.P. Dodelet, Electrochim. Acta 48 (2003) 2749.
[27] R. Jiang, F.C. Anson, J. Electroanal. Chem. 305 (1991) 171.
[28] H. Zhang, Q. Jiang, L. Sun, X. Yuan, Z. Ma, Electrochim. Acta 55 (2010) 1107.
[29] N.P. Subramanian, S.P. Kumaraguru, H. Colon-Mercado, H. Kim, B.N. Popov, T. Black, D.A. Chen, J. Power Sources 157 (2006) 56.
[30] E. Yeager, Electrochim. Acta 29 (1984) 1527.
[31] S. Ye, A.K. Vijh, J. Solid State Electrochem. 9 (2005) 146.
[32] M.S. El-Deab, T. Ohsaka, Electrochim. Acta 47 (2002) 4255.
[33] S.Lj. Gojkovic, S. Gupta, R.F. Savinell, Electrochim. Acta 45 (1999) 889.
[34] U.A. Paulus, T.J. Scmidt, H.A. Gasteiger, R.J. Behm, J. Electroanal. Chem. 495 (2001) 134.
[35] E. Claude, T. Addou, J.M. Latour, P. Aldebert, J. Appl. Electrochem. 28 (1998) 57.
[36] S. Marcotte, D. Villers, N. Guillet, L. Roué, J.P. Dodelet, Electrochim. Acta 50 (2004) 179.
[37] M. Yuasa, A. Yamaguchi, H. Itsuki, K. Tanaka, M. Yamamoto, K. Oyaizu, Chem. Mater. 17 (2005) 4278.
[38] T. Okada, M. Gokita, M. Yuasa, I. Sekine, J. Electrochem. Soc. 145 (1998) 815.
[39] K. Lee, L. Zhang, H. Lui, R. Hui, Z. Shi, J. Zhang, Electrochim. Acta 54 (2009) 4704.
[40] G. Faubert, R. Côté, J.P. Dodelet, M. Lefèvre, P. Bertrand, Electrochim. Acta 44 (1999) 2589.
[41] R.W. Reeve, P.A. Christensen, A. Hamnett, S.A. Haydock, S.C. Roy, J. Electrochem. Soc. 145 (1998) 3463.